Influence of Crystalline Properties on the Dielectric and Energy Storage Properties of Poly(vinylidene fluoride)

Junjie Li, Qingjie Meng, Wenjing Li, Zhicheng Zhang

Department of Applied Chemistry, School of Science, Ministry of Education (China) Key Laboratory for Nonequilibrium Synthesis and Modulation of Condensed Matter, Xi'an Jiaotong University, Xi'an 710049, China

Received 20 October 2010; accepted 21 December 2010
DOI 10.1002/app.34020
Published online 1 June 2011 in Wiley Online Library (wileyonlinelibrary.com).

ABSTRACT: Poly(vinylidene fluoride) (PVDF) films with various crystal phases (α, β, and γ phases) and varied crystallinities were fabricated via different processes. The influence of the crystalline properties, such as the crystallinity and crystal phases, on the breakdown strength and dielectric and energy storage properties of the films were studied. Under low electric field, the dielectric constant was governed by the crystallinities of the films, and the dielectric loss was more related to the polarity of their crystal phases. Under high electric field, the high polarity of the crystal phases favored high-maximum, remnant, and irreversible polarization of the films. The lower crystallinity of the films with the same crystal phases led to a higher maximum and remnant polarization but a lower irreversible polarization. Under direct-current electric field, the discharged energy efficiency was mainly dominated by the polar nature of crystal phases. Under an electric field below 300 MV/m, the discharged energy density and energy loss of the three kinds of films were rather close, regardless of the phase transition. When the electric field was over 300 MV/m, the overall discharged energy density was dominated by the practical breakdown strength. γ-PVDF with a proper crystallinity and crystal grain size is expected to realize an energy density over 10 J/cm^3 under an electric field over 400 MV/m. © 2011 Wiley Periodicals, Inc. J Appl Polym Sci 122: 1659–1668, 2011

Key words: crystallization; dielectric properties; fluoropolymers

INTRODUCTION

Poly(vinylidene fluoride) (PVDF), as a semicrystalline polymer, exhibits interesting physical and electrical properties, depending on its molecular weight, molecular weight distributions, chain conformations, crystalline form, and even defects of chaining.[1] It has been well studied and applied in a wide range since its attractive piezoelectric,[2] pyroelectric,[3,4] and ferroelectric[5] properties were first discovered. These properties are mostly related to the β-crystalline form of PVDF, which has a zigzag (all-trans) conformation (TTT) of the polymer chain and could be obtained by straining, stretching, quenching, or polarizing under a high electric field.[6] Besides the β-crystalline form with strong polarization, PVDF has at least the other four crystalline forms, including α, γ, δ, and ε phases, depending on the fabrication processes and conditions, which have been well documented in the literature.[7,8] The nonpolar α-phase PVDF, having a trans–gauche conformation (TGTG′), is the most popular one, which can be normally obtained by melt crystallization at temperatures below 160°C.[9] The intermediately polar γ phase, consisting of a parallel packing of TTTG conformation, can be obtained by annealing of the α-phase PVDF at about 157°C or moderate stressing. The δ phase is a polar version of the α phase and is obtained by the polarization of an originally α-phase sample in an electric field of 125 MV/m. The ε phase is reported as a reverse version of the δ phase and can be produced by annealing of the δ-phase PVDF at high temperature.[10] Both δ- and ε-PVDF are rarely studied because of their poor stabilities.

Recently, PVDF-based fluoropolymers have been used to prepare high-pulse discharge capacitors for their high-energy storage capabilities and have attracted considerable research interest.[11–19] Among these cases, the most successful one was the modification of vinylidene fluoride (VDF) and trifluoroethylene copolymer via chemical incorporation of a third monomer (chlorotrifluoroethylene or chlorodifluoroethylene)[20] as kinks to tailor the polar TTT conformation of poly(vinylidene fluoride-*co*-trifluoroethylene) into the TTTG conformation of poly[vinylidene fluoride-*co*-trifluoroethylene-*co*- chlorotrifluoroethylene

Correspondence to: Z. Zhang (zhichengzhang@mail.xjtu.edu.cn).

Contract grant sponsor: National Natural Science Foundation of China; contract grant number: 50903065.

Contract grant sponsor: Scientific Research Foundation for the Returned Overseas Chinese Scholars, State Education Ministry.

(chlorodifluoroethylene)] with weaker polarity. As a result, the dielectric constant (ε_r') and energy density of the resulting terpolymer with an optimized composition were obtained as high as 100 and 13 J/cm^3,[13] respectively. Furthermore, the uniaxial stretching of VDF/chlorotrifluoroethylene (91/9 mol %)[15] and VDF/hexafluoropropene (95.5/4.5 mol %)[18,19] copolymers could be used to prepare more promising dielectric films with energy densities over 25 J/cm^3 under 600 and 700 MV/m electric field, respectively. In these cases, the polarity weakening of the polymer chain conformation (from a high-polar β phase to a weakly polar γ phase or nonpolar α phase) and the reduction of the crystalline properties has accounted for the dramatic improvement of their dielectric properties. The widely accepted fundamental idea of improving the energy density of PVDF-based fluoropolymer is the reduction of the polarity of the crystal domains to enhance the applied electric field and a decrease in the crystal grain size to improve the energy-discharging efficiency of the dipole moments. However, the incorporation amount and even the inserting defect of comonomers would reduce the overall dipole moments of the final material,[16] which govern the energy storage capabilities. Therefore, all of the copolymers obtained from modified PVDF possess lower energy storage capabilities than that of neat PVDF. Simultaneously, these copolymers are too complicated because of their wide composition distribution to understand how the crystalline properties influence their dielectric and energy storage properties exactly.

In an effort to illuminate the crystalline properties dependence on the dielectric and energy storage properties of PVDF-based fluoropolymers more clearly, three kinds of PVDF films with various crystalline phases, including α, β, and γ phases, and varied crystallinities and crystal domain sizes are presented in this work. The effects of the crystalline phase, crystallinities, and crystal domain size on the dielectric and energy storage properties of PVDF were carefully investigated. Although the dielectric relaxation properties of α- and β-PVDF have been well reported previously,[21–28] the dielectric properties of γ-PVDF and the energy storage properties of PVDF have rarely been mentioned so far.

EXPERIMENTAL

Materials

PVDF (SOLEF6010), in powder with a weight-average molecular weight of 300,000, was supplied by Solvay Solexis (Brussels, Belgium). The uniaxially stretched β-PVDF film (30 μm thick) coated with aluminum on both sides as an electrode was purchased from Jinzhou Kexin Dianzi Cailiao Co., Ltd. The other chemicals were obtained from commercials and were used as received.

Fabrication of the PVDF films with different crystalline properties

PVDF films (20–30 μm) in the α-phase crystal domain were prepared via casting of the PVDF solution in dimethylformamide on a glass substrate followed by drying at 100°C for 24 h. The obtained films were peeled from the substrate and marked as untreated α-PVDF. The untreated α-PVDF films together with the glass substrates were heated at 200°C for 30 min followed by immediate merging into an ice-water bath (quenched α-PVDF) or gradual cooling to room temperature in an oven for 24 h (annealed α-PVDF).

Untreated γ-PVDF films were prepared via the casting of the PVDF solution in dimethylformamide at 40°C. The obtained γ-PVDF films were heated at 180°C for 5 min; this was followed by immediate quenching in an ice-water bath (quenched γ-PVDF) or gradual cooling in an oven for 24 h (annealed γ-PVDF). γ-PVDF films could not be kept at high temperature for too long; otherwise, the crystal phase would be turned into an α phase.

Characterization

X-ray diffraction (XRD) analysis was conducted on a Rigaku D/MAX-2400 (Rigaku Industrial Corp., Tokyo, Japan). Differential scanning calorimetry (DSC) analysis was conducted on a Netzsch DSC 200 PC (Netzsch Corp., Selb, Germany) in a nitrogen atmosphere at a heating speed of 10°C/min. For electric characterizations, gold electrodes (ca. 50 nm) were sputtered on both surfaces of the α- and γ-PVDF films. A polarized optical micrograph was obtained under crossed polarizers with an XP600 (Shanghai Wanheng Corp., China) at room temperature. The photographs for the sample films were taken with a Nikon Coolpix 5600 digital camera equipped on the vertical hood of the optical microscope. The ε_r' and dielectric loss (tan δ) of the polymers were acquired with an HP multifrequency LCR meter (HP 4284A) scanned at increasing frequency from 50 Hz to 10 MHz with a 1-V bias voltage. The electric displacement–electric field (D–E) hysteresis loops were measured on a modified Sawyer–Tower circuit and a linear variable differential transducer driven by a lock-in amplifier (Stanford Research Systems, model SR830). The discharged energy density and energy loss of the polymers were calculated from their unipolar D–E loops, as described in the literature.[16] We measured the dielectric breakdown strength with a dielectric strength tester (CJ2671) (Nanjing Changjiang Radio

TABLE I
DSC, XRD, and FTIR Results of PVDF with Different Crystalline Properties

PVDF	2θ from XRD (°)	Wave number from FTIR (cm^{-1})	DSC		
				Melting temperature (°C)	ΔH (J/g)
α phase	17.9 (110), 18.4 (020), 20.2 (021), 27.9 (111), 36.1 (200), 39.0 (002)	408, 532, 614, 764, 796, 855, 976	Untreated	173.0	58.6
			Quenched	173.6	39.8
			Annealed	174.6	60.3
β phase	20.7 (110, 200), 36.6 (020, 101), 56.9 (221)	444, 512, 776, 812, 833, 840	Stretched	167.4	41.0
γ phase	18.5 (020), 20.1 (110), 38.7 (211)	431, 484, 512, 776, 812, 840	Untreated	174.9	53.2
			Quenched	174.2	44.3
			Annealed	173.4	56.1

Factory, China) by sweeping the applied voltage from 0 at approximately 1 kV/min until the point of catastrophic device failure, as evidenced by spurious current changes and the pitting of the top electrode.

RESULTS AND DISCUSSION

Characterization of the PVDF films with different crystal phases [XRD, DSC, Fourier transform infrared (FTIR) spectroscopy, and polarimeter microscopy]

Table I presents the XRD and FTIR results and their assignments of the PVDF films with three different crystal phases. In the α-PVDF films, the peaks at 2θ = 17.9, 18.4, 20.2, 27.9, 36.1, and 39.0° were assigned to the (110), (020), (021), (111), (200), and (002) reflections of the α-phase crystal plane, respectively. In the γ-PVDF films, the peaks at 18.5, 20.1, and 38.7° were the (020), (110), and (211) reflections of the γ-phase crystal plane, respectively. In the uniaxially stretched film, the peak at 20.7° was assigned to the (110, 200) reflection, the peak at 36.6° was assigned to the (020, 101) reflection, and the peak at 56.9° corresponded to the (221) reflection of the β-PVDF crystal plane.[29] The same conclusion could also be obtained from FTIR spectroscopy, as shown in Figure 1 and Table I. In the α-PVDF films, the α phase could be confirmed by the characteristic absorption bands at 408, 532, 614, 764, 796, 855, and 976 cm^{-1}. The absorption bands at 431, 512, 776, 812, 833, and 840 cm^{-1} observed in the γ-PVDF film were characteristic of the γ-phase PVDF,[30] which confirmed the majority of γ-phase crystals in this film. The bands at 444, 512, and 840 cm^{-1} were regarded as characteristic of the β phase.[31] Meanwhile, the peaks at 614 and 796 cm^{-1} were characterized as typical of α-PVDF; this indicated the existence of minor α phase in the β-PVDF film. All of the information indicated that the samples obtained possessed the majority of the corresponding crystal phase, as desired.

Figure 2 presents the XRD spectra of the α- and γ-PVDF films treated in different thermal processes. Their XRD spectra showed little difference, which indicated that different thermal treatment processes exhibited little influence on the crystal forms of the films. However, the size of the crystal domain and the *d*-spacing of the microcrystal in the films were greatly influenced. As shown in Figure 2, the *d*-spacings of (110), (020), and (021) reflections in the α-PVDF films at 2θ = 17.9, 18.4, and 20.2° were 4.94, 4.82, and 4.39 Å, respectively. In both the untreated and quenched α-PVDF films, a (020) reflection with lower *d*-spacing could be observed, whereas the (020) reflection disappeared and was displaced by the (110) reflection at 2θ = 17.9° in the annealed samples; this suggested the improvement of the crystal domain. This could also be confirmed by the morphology of the crystal domain in the α-PVDF films; this was measured with polarized optical microscopy because their spherical crystal grains would exhibit back-cross under polarized optical microscopy. As shown in Figure 3, several large

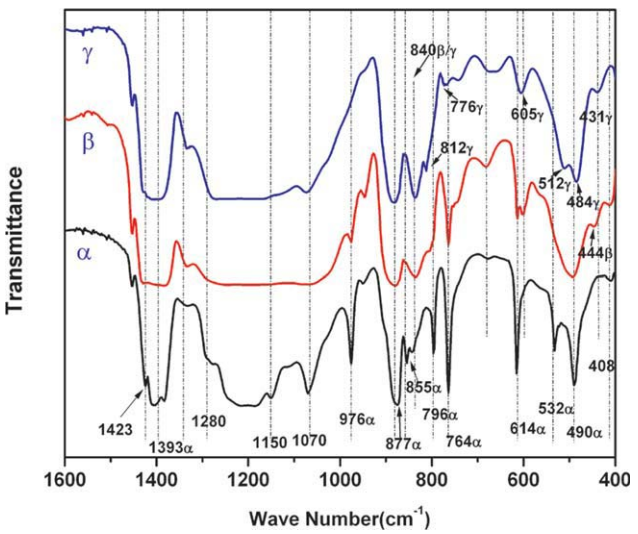

Figure 1 FTIR and assignment of PVDF in α-, β-, and γ-form crystal phase. [Color figure can be viewed in the online issue, which is available at wileyonlinelibrary.com.]

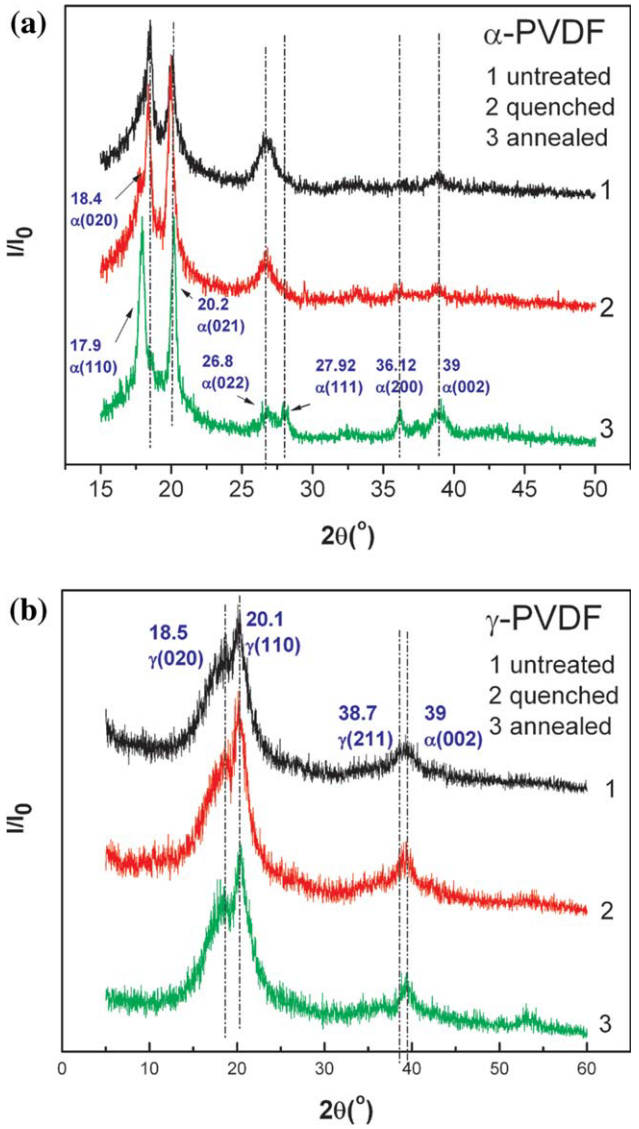

Figure 2 XRD and assignment of α- and γ-PVDF films treated in different thermal processes. The relative intensity I/I_0 is the peak height of the diffraction peak divide by the strongest diffraction peak and then multiplied by 100. [Color figure can be viewed in the online issue, which is available at wileyonlinelibrary.com.]

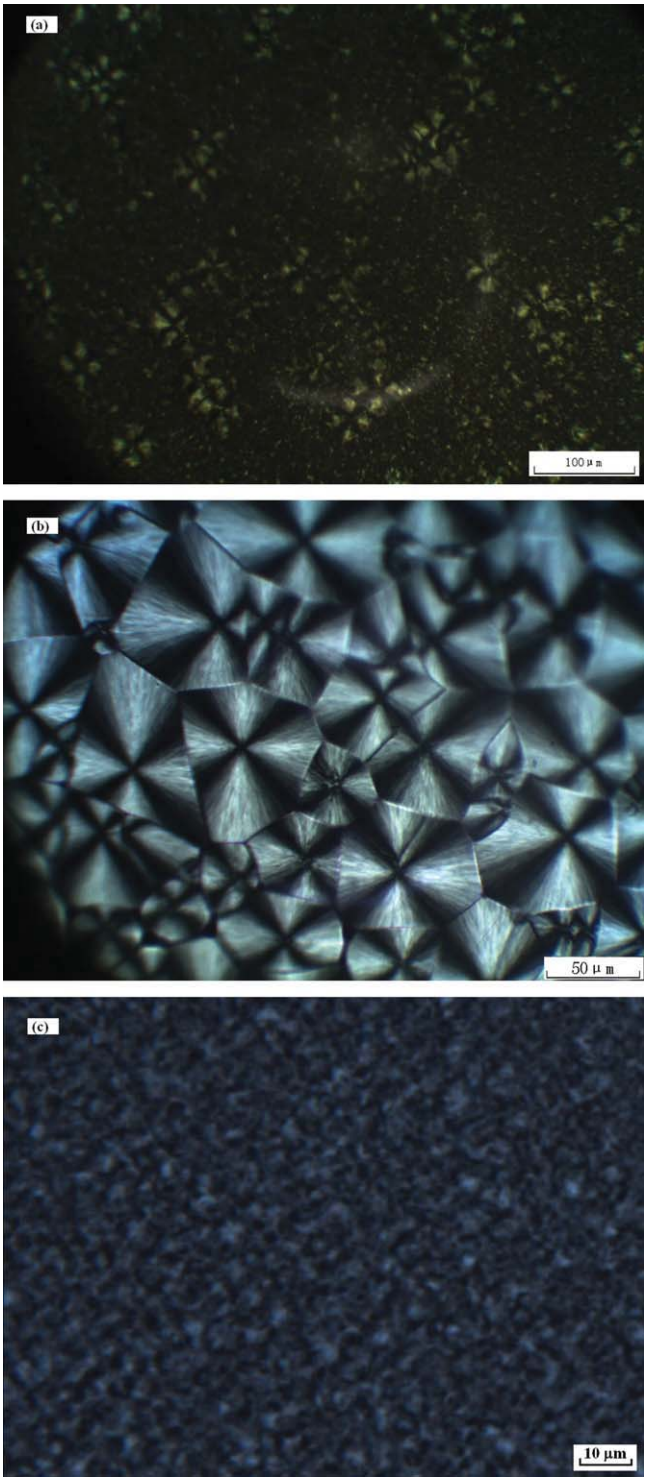

Figure 3 Morphology of crystal domains of (a) untreated, (b) annealed, and (c) quenched α-PVDF films. [Color figure can be viewed in the online issue, which is available at wileyonlinelibrary.com]

crystal grains scattered in the untreated α-PVDF films are observed, whereas the whole film filled with crystal grains in larger scale were observed in the annealed α-PVDF. The crystal domain size of the quenched α-PVDF film was less than 10 μm, which was too small to be observed even when it was magnified 600×. Meanwhile, thermal treatments may have altered the crystallinity of the polymer as well. Annealing could slightly improve the crystallinity of the films, which was evidenced by an in increase in the heat of fusion, as shown in Table I. Quenching in ice-water resulted in a great reduction of the heat of fusion in DSC (e.g., from 58.6 to 39.8 J/g in the α-PVDF and from 53.2 to 44.3 J/g in the γ-PVDF); this indicated the decreasing of crystallinity. In general, the film fabrication methods governed the crystal phase of the PVDF films, whereas the thermal treatment mainly affected the crystallinity and the size of crystal domain.

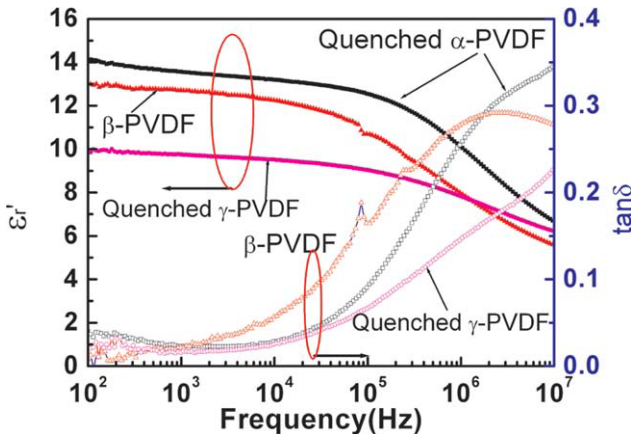

Figure 4 ε_r' and loss of PVDF in different crystal phases. (Both the α- and γ-PVDF films were quenched). [Color figure can be viewed in the online issue, which is available at wileyonlinelibrary.com]

Dielectric relaxation of the PVDF films with different crystalline properties

Figure 4 presents ε_r' and tan δ of PVDF in different crystal phases measured in a low electric field (bias voltage = 1 V) with increasing frequency. As the frequency increases, ε_r' of all of the films decreased because they were ferroelectric and nonlinear in nature. The ε_r' of the three PVDF films in a 100-Hz electric field was in the order of α-PVDF (∼ 14) > β-PVDF (∼ 13) > γ-PVDF(∼ 10). ε_r' of both α- and β-PVDF against the electric field frequency exhibited a sharp reduction at about 100 kHz, whereas ε_r' of γ-PVDF showed little variation as the frequency increased from 100 Hz to 10 MHz. Under low electric fields, ε_r' mostly reflected the mobility of the dipole moments in the amorphous phase and small crystal domains. Among these three samples, the quenched α-PVDF had the lowest crystallinity (heat of fusion (ΔH) of α-PVDF obtained from DSC is 39.8 J/g) and smaller crystal domain; therefore, the response of the dipole moment was the highest. The lowest ε_r' observed in γ-PVDF was attributed to its relatively high crystallinity (ΔH = 44.3 J/g) and large crystal domain, thanks to the slow crystallization process at low temperature (∼ 40°C). The fact that ε_r' of stretched β-PVDF was between that of α- and γ-PVDF could be accounted for by its medial crystallinity (ΔH = 41.0 J/g) and high polarity of polymer chains.

As shown in Figure 4, the γ-PVDF and β-PVDF films exhibited the lowest and the highest tan δ values among the three samples in the range of 1 kHz to 1 MHz, respectively. At a high frequency (∼ 1 MHz), two molecular motions, the micro-Brownian motion of noncrystalline chain segments (β relaxation) and the molecular motion onto the amorphous/crystalline interfaces,[32] have been proposed to be responsible for the relaxation process. For these three samples, quenched α-PVDF, stretched β-PVDF, and quenched γ-PVDF, the heats of fusion obtained from DSC were 39.8, 41.0, and 44.3 J/g, respectively. That means the contribution of noncrystalline chain segments of these samples was rather close because their crystallinities were similar. Apparently, their different relaxation behaviors under low electric field were more related to the second reason, namely, the molecular motion onto the amorphous/crystalline interfaces. The γ-PVDF film produced from a low-temperature solution casting process exhibited the lowest relaxation response because it had only a flat-on large crystal and, therefore, the lowest amorphous/crystalline interfaces. This was already confirmed in a poly(vinylidene fluoride-*co*-hexafluoropropene) copolymer.[18] The quenched high-temperature, solution-cast film (α-PVDF) and the uniaxially stretched (β-PVDF) film possessed smaller crystal domains and more interface areas between the amorphous and crystalline regions. Therefore, their corresponding relaxation response was higher than that of the low-temperature, solution-cast γ-PVDF at high frequency. Meanwhile, the different relaxation responses of the interfaces between the PVDF crystal domain in the different crystal phases and amorphous domains could be speculated as another important reason. Apparently, the relaxation response of the PVDF crystal domain with a higher polarity (β phase) was larger than that with a lower polarity (α and γ phase), and the relaxation peak appeared at lower frequency correspondingly.

Besides the crystal phase, the crystallinity and crystal domain size showed a dominant influence on the ε_r' and tan δ of PVDF under low electric field; even their crystal phases were the same. As shown in Figure 5, thermal treatment led to a significant influence on the ε_r' of α- and γ-PVDF. The ε_r' of the α-PVDF samples was in the order of quenched > untreated > annealed, and that of the γ-PVDF films was in the order of quenched > untreated, which was the same as the order of ΔH and the crystallinity of the corresponding samples. That means the ε_r' under low electric field was more related to the amorphous phase and microcrystal domain in the films. Apparently, the quenched samples with lower crystallinity exhibited a higher dielectric response, whereas annealing favored the crystalline phase and, therefore, a low dielectric response. However, the dielectric loss was weakly affected by the thermal treatments, even at high frequency. As shown in Figure 5, the dielectric loss curves of the three α-PVDF and two γ-PVDF films against frequency are rather close. Only a slight difference was observed over 1 MHz; the order was quenched > untreated > annealed α-PVDF. This suggests that the interface

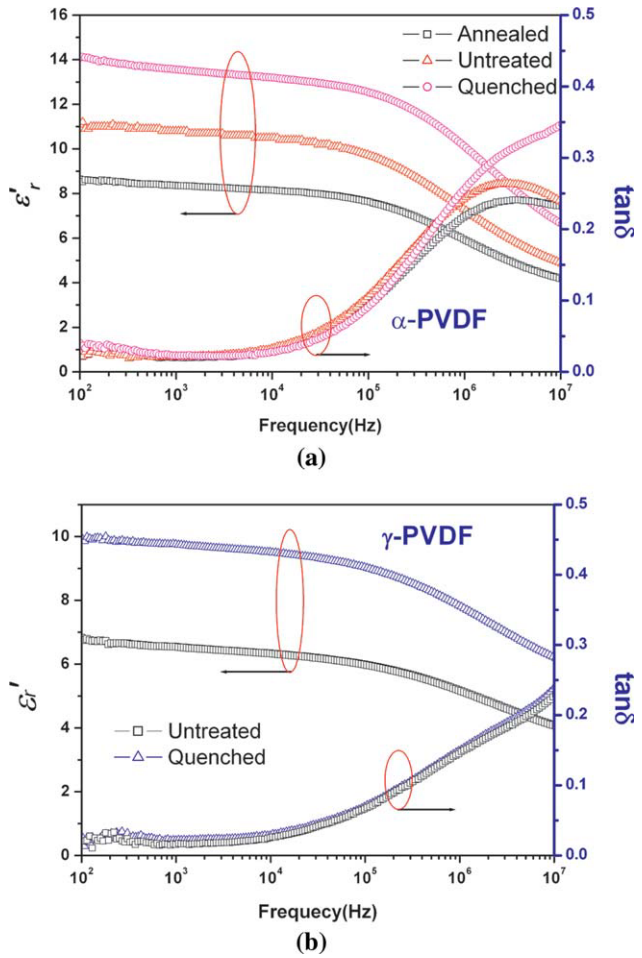

Figure 5 Thermal treatment dependence of ε_r' and tan δ of α- and γ-PVDF. [Color figure can be viewed in the online issue, which is available at wileyonlinelibrary.com]

areas between the crystal and amorphous phases showed a very limited influence on the relaxation response of the film. That further confirmed that the crystal phase with varied polarity, as discussed previously, was the dominant factor in the different relaxation responses of the PVDF films.

D–E hysteresis loops of PVDF

Figure 6 presents the D–E loops of PVDF with three different crystal forms measured under alternating-current and direct-current electric field at 10 Hz, respectively. The dipolar D–E loops of α-PVDF under the electric field less than 200 MV/m was oval in shape, and the curves became fatter with the increase of electric field. Once the electric field was over 300 MV/m, the oval-shape loop turned into near parallelogram. It has been discussed that the high electric field may have induced the α to γ phase transition of PVDF even at room temperature, and the phase transition happened gradually as the electric field increased.[33] That means it was not possible to measure the D–E loops of neat α-PVDF under high electric field because more or less α-PVDF would have been transferred into γ phase. The evidence that dipolar D–E loops of α- and γ-PVDF under a 300 MV/m electric field were rather similar, as shown in Figure 6(a,b), also confirmed the

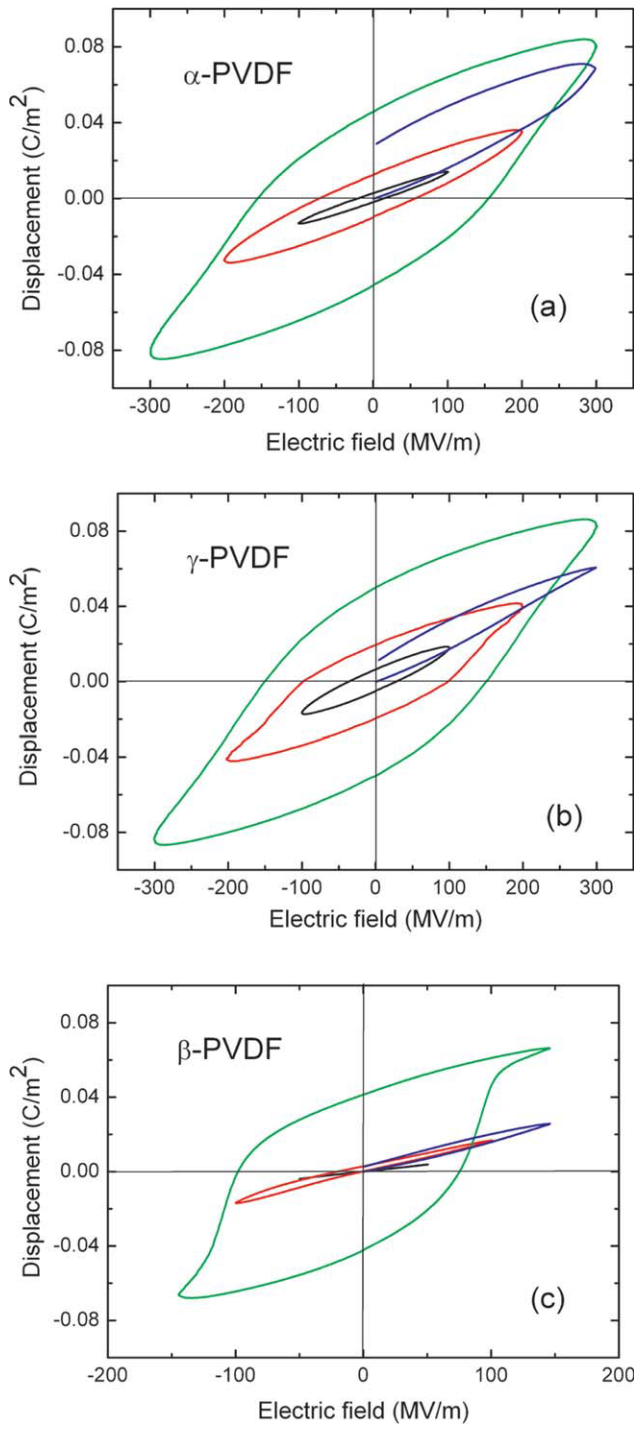

Figure 6 Unipolar and dipolar D–E hysteresis loops of α-, β-, and γ-PVDF films. [Color figure can be viewed in the online issue, which is available at wileyonlinelibrary.com]

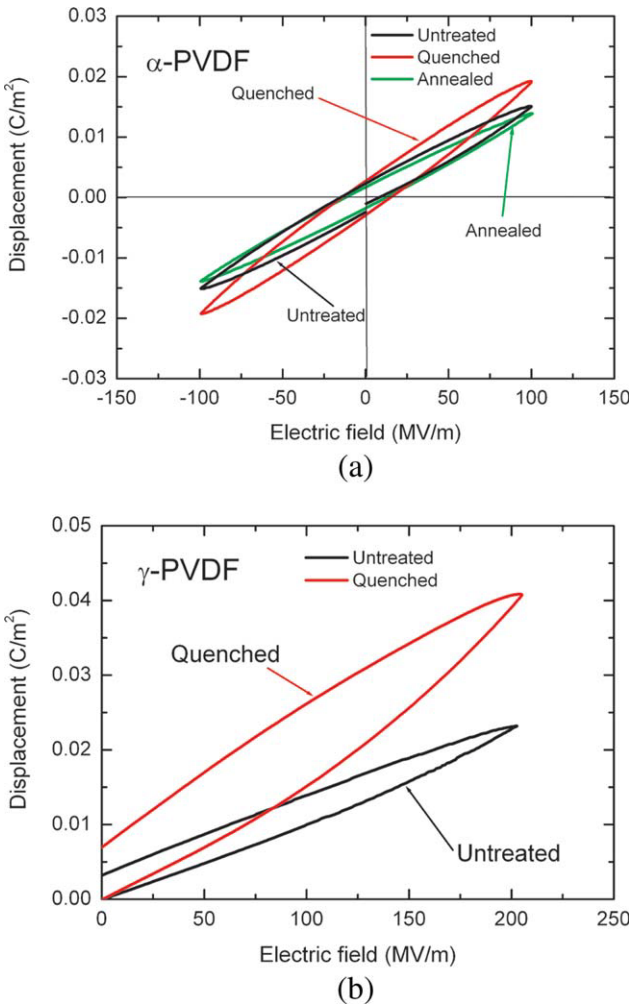

Figure 7 Thermal treatment dependence of D–E loops of α- and γ-PVDF films. [Color figure can be viewed in the online issue, which is available at wileyonlinelibrary.com]

conclusion. The major difference between the α- and γ-PVDF dipolar D–E loops was under an electric field of less than 300 MV/m. Generally, γ-PVDF possesses slightly higher maximum and remnant polarization than that of α-PVDF for its weakly higher polarity of TTTG chain conformation. This could also have accounted for the truth that the D–E loop of γ-PVDF under 200 MV/m was already in near parallelogram shape, whereas the D–E curve of α-PVDF was still an oval shape. Another difference between α- and γ-PVDF was the irreversible polarization under a high electric field, which could be calculated by subtraction of unipolar remnant polarization from the dipolar remnant polarization. Under a 300 MV/m electric field, the irreversible polarization of γ-PVDF was as high as 60% of overall remnant polarization, whereas that of α-PVDF was only about 30%. Besides the slightly higher polarity of γ-PVDF over that of α-PVDF, the less amorphous/crystalline interface areas of γ-PVDF compared to those of α-PVDF, discussed previously, could be speculated as another reason, which may have delayed the reversal of the aligned crystal domains.

β-PVDF exhibited typical ferroelectric properties under increasing electric field, as shown in Figure 6(c). When the applied electric field was lower than its coercive field (ca. 100 MV/m), the D–E loops obtained were in slim linear, and both the maximum and remnant polarizations were rather low. If the applied field was over the coercive field (e.g., 150 MV/m), both the maximum and remnant polarizations increased sharply, and the D–E curve turned into near rectangle shape. Further slight increases in the applied field (ca. 300 MV/m) led to polarization saturation immediately, which was mainly dominated by the high polarity of β-PVDF in the all-trans chain conformation. A low electric field could only polarize the microcrystal and amorphous dipoles, whose contents were rather low, and most of them are reversible for their small size. When the electric field was sufficiently high to orient the large polar crystal grain, the displacement would have been improved dramatically. However, most of the oriented large crystal could not be disoriented freely because the free space between the crystal grains was not sufficient for their disordering. Therefore, the remnant polarization was quite high, and most of the polarization (>80%) was irreversible.

Besides the crystal-phase forms, crystallinity exhibited great influence on the D–E loops of PVDF as well. D–E hysteresis loops of α- and γ-PVDF with varied crystal phases and crystallinities are presented in Figure 7. Generally, the maximum polarization and remnant polarization of α-PVDF were in the order of quenched > untreated > annealed, and those of γ-PVDF were in the order of quenched > untreated, which was the opposite order of their crystallinities. As discussed previously, quenching may reduce the crystallinity and the size of crystal domain. The microcrystal domain and amorphous dipoles were more easily poled under low electric fields. However, their disorientation was random and took a longer period to relax completely; this was evidenced as the reduction of the remnant polarization with decreasing testing frequency.[26] As a result, both the maximum and remnant polarization improved as their crystallinity decreased. Meanwhile, the irreversible polarization was reduced as the amorphous phase increased because the crystal size was reduced, and more free space was provided for the flipping of the crystal domains. The big success obtained in the modification of ferroelectric poly(vinylidene flouride–trifluoroethylene) either with the electron irradiation[34] or chemical copolymerization method[20] to reduce the crystal size and increase the amorphous phase content also confirmed this. It is reasonable to believe

TABLE II
Breakdown Strength, Energy Density, and Loss of PVDF

Sample	α-PVDF			β-PVDF	γ-PVDF		
	Annealed	Untreated	Quenched	Stretched	Annealed	Untreated	Quenched
Breakdown strength (MV/m)	322.1	261.5	331.8	306.0	412.0	395.3	400.7
Energy density (J/cm^3)	4.6	2.7	6.8	5.6	6.9	7.4	9.5
Energy loss (J/cm^3)	6.1	6.7	7.8	2.9	4.0	4.3	5.7
Efficiency (%)	43.0	28.7	46.6	65.9	63.3	63.2	62.5

that reducing the crystallinity of β-PVDF via an adaptable treatment process could effectively decrease its irreversible polarization as well.

Breakdown strength and energy storage of PVDF

It has been predicted that the maximum polarization of single-crystal β-PVDF is about 0.13 C/m^2.[35] That means all the dipoles are aligned in parallel along the electric field direction when the maximum polarization is reached, which is named *displacement saturation* as well. To achieve a high energy density, a high electric field must be allowed to be applied; this is as important as high saturation polarization based on the calculation method ($U_e = \int E_d D$, where U_e is the energy density, E is the breakdown electric field, D is the displacement, and d is the partial differential symbol) described in literature.[16] Apparently, the saturation electric field is another limitation for high-energy storage purposes because no more energy could be stored as soon as the displacement saturation is reached. Following the discussion about the D–E loops, the saturation electric field of low-polar α- and γ-PVDF should have been the same with respect to the phase transition occurring under electric fields over 300 MV/m, and both of them were much higher than that of high-polar β-PVDF (∼ 200 MV/m). That means α- and γ-PVDF should be applied under higher electric fields than β-PVDF.

However, the dielectric films usually have already been broken before they reach displacement saturation because of the flaws or defects in the films during the film fabrication process. Therefore, the breakdown strength has more practical meanings than the saturation electric field. The average breakdown electric fields of PVDF films with different crystalline properties fabricated in this work were tested and are presented in Table II. The average breakdown electric field of the α-PVDF films was below 350 MV/m, which was slightly higher than that of the uniaxially stretched β-PVDF films (ca. 300 MV/m) and lower than that of γ-PVDF (ca. 400 MV/m). It has been well discussed that the phase transition from the α to the γ phase would happen in α-PVDF under an electric field from 200 to 350 MV/m. That means the polymer chain in the crystal phase would be tuned from TGTG′ to the TTTG conformation, and one of every four VDF units must be twisted for a certain angle. Therefore, the breakdown strength of the α-PVDF films was dominated by both the uniformity of the crystal grains in the films and the phase-transition electric field. For annealed α-PVDF films, the phase transition could hardly have been accomplished because of the low free space provided by the amorphous phase. Therefore, the films were usually broken below 350 MV/m (∼ 320 MV/m). For the untreated α-PVDF films, the poor uniformity of crystal grains in the films [as shown in Fig. 3(a)] led to a rather low breakdown electric field (∼ 260 MV/m). The phase transition had more chances to be accomplished in quenched α-PVDF films for the high free space provided by the relatively high content of amorphous phase. Meanwhile, quenching also favored the formation of microcrystal grains and the uniformity of the crystal domains in the films; therefore, the breakdown electric field was the highest (∼ 330 MV/m). Apparently, increasing the uniformity and decreasing the crystal size were crucial for enhancing the breakdown strength of the α-PVDF films. For β-PVDF, stretching gave its high uniformity of crystal grains in the films. However, the polarization saturation limited the further improvement of the electric field. As a result, its breakdown electric field (∼ 300 MV/m) was rather close to the polarization saturation field. For the γ-PVDF films, neither the phase transition nor polarization saturation happened under electric fields of less than 600 MV/m. Therefore, the key to enhancing their breakdown field was improving the uniformity of the films. The slow evaporation of solvent at low temperature (∼ 40°C) allowed the crystal grain to grow evenly. Thus, the untreated γ-PVDF films had breakdown strengths as high as 395 MV/m. The following annealing and quenching were able to further improve the uniformity of the films and the breakdown electric field (>400 MV/m).

The discharged energy density, energy loss, and energy discharged efficiency of the PVDF films under the corresponding breakdown electric fields

were calculated from the unipolar D–E loops and are listed in Table II. The energy discharged efficiency is the percentage of discharged energy in the overall energy charged and is calculated via division of the energy density by the sum of the energy density and loss. As shown in Table II, the energy density and efficiency of the α-PVDF films were in the order of quenched > annealed > untreated. The different maximum polarization and remnant polarization of varied films under the same electric field were responsible for this result. A high maximum polarization and low remnant polarization would have led to a high energy density and low energy loss, which was consistent with the unipolar D–E curves of the α-PVDF films, as discussed previously. The extremely low discharged energy density and efficiency of the untreated α-PVDF film may have been to the slow disorientation of polarized crystal grains in these films for their poor uniformity of crystal grains. For γ-PVDF, the energy efficiency of all of the films was around 63%; this means that thermal treatment did not show an obvious effect on it. However, the energy density of the γ-PVDF films was in the order of quenched > untreated > annealed, which was in the opposite order of their crystallinities. That means more energy would have been charged and discharged if the crystal grain size and crystallinity of the films were reduced; this confirmed the results, as discussed previously, that a higher polarization was obtained in the films with lower crystallinity. The discharged energy efficiency with respect to the influence of the different crystal phases was in the order of β-PVDF (∼ 66%) > γ-PVDF (∼ 63%) > α-PVDF (∼ 47% for quenched films), which was the same as the polar nature of the different crystal phases. That means the disorientation ability of the PVDF crystal grains was more related to their polarities. The crystal domains with higher polarity may have disordered more quickly, regardless of the irreversible polarization. The crystallinity of the β-PVDF film and the quenched α- and γ-PVDF measured with DSC was rather close, as discussed previously. This allowed us to speculate the different energy densities obtained in these three samples to the various crystal phases. We just reported[32] that both the energy density and loss of these three PVDF films were rather close under a low electric field (<300 MV/m). However, it was not possible to fairly compare the energy storage ability of three kinds of PVDF films under electric fields over 300MV/m because the phase transition or displacement saturation in the α- and β-PVDF was induced by the electric field. As a matter of fact, the breakdown electric field became the dominant factor for the energy density of different films under a high electric field.

CONCLUSIONS

In this study, three kinds of PVDF films with α-, β-, and γ-phase crystal domains and varied crystallinities were fabricated via different processes. The thermal treatments showed little influence on their crystal phases; this was related to the dielectric loss, but the treatments had great effects on their crystal grain sizes and crystallinities, which mainly determined the ε_r' under a low electric field. Under a high electric field, the higher crystal phase and low crystallinity precipitated a higher maximum and remnant polarization. The γ-PVDF films had the highest breakdown strength, around 400 MV/m, among the three kinds of films because the α- and β-PVDF films were limited by the phase transition and displacement saturation. The discharged energy density was governed by the breakdown strength and the effective polarization. γ-PVDF films with certain low crystallinity and crystal grain size were expected to realize over 10 J/cm^3 of discharged energy density under an electric field of 400 MV/m, which was several times higher than Biaxially Oriented Polypropylene (BOPP).

References

1. Bovey, F. A.; Jelinski, L. W. Chain Structure and Conformation of Macromolecules; Academic: New York, 1982.
2. Kawai, N. Jpn J Appl Phys 1969, 8, 1975.
3. Bergman, J. G.; McFree, J. H.; Crane, G. R. Appl Phys Lett 1971, 18, 203.
4. Nakamura, K.; Wada, Y. J Polym Sci Part A-2: Polym Phys 1971, 9, 161.
5. Lovinger, A. Science 1983, 220, 1115.
6. Nasef, M. M.; Saidi, H.; Dahlan, K. Z. M. Polym Degrad Stab 2002, 75, 85.
7. Nalwa, H. S. Ferroelectric Polymers: Chemistry, Physics and Applications; Marcel Dekker: New York, 1995.
8. Lovinger, A. J. Developments in Crystalline Polymers; Basset, D. C., Ed.; Applied Science: London, 1982.
9. Bachman, M. A.; Lando, J. B. Macromolecules 1981, 14, 40.
10. Lovinger, A. J. Macromolecules 1982, 15, 40.
11. Chu, B. J.; Zhou, X.; Ren, K. L.; Neese, B.; Lin, M. R.; Wang, Q.; Bauer, F.; Zhang, Q. M. Science 2006, 313(5785), 334.
12. Chu, B. J.; Zhou, X.; Neese, B.; Zhang, Q. M.; Bauer, F. IEEE Trans Dielectr Electr Insul 2006, 13, 1162.
13. Zhang, Z. C.; Chung, T. C. M. Macromolecules 2007, 40, 783.
14. Zhang, Z. C.; Chung, T. C. M. Macromolecules 2007, 40, 9391.
15. Zhou, X.; Chu, B. J.; Neese, B.; Lin, M. R.; Zhang, Q. M. IEEE Trans Dielectr Electr Insul 2007, 14, 1133.
16. Zhang, Z. C.; Meng, Q. J.; Chung, T. C. M. Polymer 2009, 50, 707.
17. Guan, F. X.; Yuan, Z. Z.; Shu, E. W.; Zhu, L. Appl Phys Lett 2009, 94, 052907.
18. Guan, F. X.; Pan, J. L.; Wang, J.; Wang, Q.; Zhu, L. Macromolecules 2010, 43, 384.
19. Zhou, X.; Zhao, X. H.; Suo, Z. G.; Zou, C.; Runt, J.; Liu, S.; Zhang, S. H.; Zhang, Q. M. Appl Phys Lett 2009, 94, 162901.
20. Chung, T. C.; Petchsuk, A. Macromolecules 2002, 35, 7678.
21. Gregorio, R.; Ueno, E. M. J Mater Sci 1999, 34, 4489.

22. da Silva, A. B.; Wisniewski, C.; Esteves, J. V. A.; Gregorio, R. J Mater Sci 2010, 45, 4206.
23. Belouadah, R.; Kendil, D.; Bousbiat, E.; Guyomar, D.; Guiffard, B. Phys B 2009, 404, 1746.
24. Nagai, M.; Nakamura, K.; Uehara, H.; Kanamoto, T.; Takahashi, Y.; Furukawa, T. J Polym Sci Part B: Polym Phys 1999, 37, 2549.
25. Li, X.; Chen, S. T.; Yao, K.; Tay, F. E. H. J Polym Sci Part B: Polym Phys 2009, 47, 2410.
26. Hughes, O. R. J Polym Sci Part B: Polym Phys 2007, 45, 3207.
27. Zheng, J. P.; Cygan, P. J.; Jow, T. R. IEEE Trans Dielectr Electr Insul 1996, 3, 144.
28. Ozkazanc, E.; Guney, H. Y.; Oskay, T.; Tarcan, E. J Appl Polym Sci 2008, 109, 3878.
29. Esterly, D. M.; Love, B. J. J Polym Sci Part B: Polym Phys 2004, 42, 91.
30. Weinhold, M.; Litt, M. H.; Lando, J. B. J Polym Sci Polym Phys Ed 1979, 17, 585.
31. Enomoto, S.; Kawai, Y.; Sugita, M. J Polym Sci Part A 1968, 22, 861.
32. Furukawa, T; Wang, T. In The Applications of Ferroelectric Polymers; Wang, T., Herbert, J. M., Glass, A. M., Eds.; Chapman & Hall: New York, 1988; Vol. 5, p 66.
33. Li, W. J.; Meng, Q. J.; Zheng, Y. S.; Zhang, Z. C.; Xia, W. M.; Xu, Z. Appl Phys Lett 2010, 96, 192905.
34. Zhang, Q. M.; Bharti, V.; Zhao, X. Science 1998, 280(5372), 2101.
35. Al-Jishi, R.; Taylor, P. L. J Appl Phys 1985, 57, 902.